Effect of Kinetics and Mass Transfer on Design of Extractive Reaction Processes

Ketan D. Samant and Ka M. Ng
Dept. of Chemical Engineering, University of Massachusetts, Amherst, MA 01003

A generic model is derived for studying the effects of chemical kinetics and mass transfer on extractive reaction processes. Activity-based models are used to describe nonideal liquid-liquid phase equilibrium and reaction kinetics. Maxwell-Stefan formulation and the film model are used to describe multicomponent mass transfer. The effects of kinetics and mass transfer are described in terms of Damköhler number matrices for reaction and for mass transfer, respectively. The elements of these matrices measure the rates of reactions and mass transfer relative to product removal. These effects are demonstrated using examples of systems with inherent phase separation and systems with solvent-induced phase separation. The results show that it may not always be beneficial to operate extractive reaction processes near the equilibrium thermodynamic limit. Damköhler numbers have to be chosen carefully to obtain the desired performance. The use of the model in evaluating performance trade-offs and in making judicious choices about reactor attributes is demonstrated.

Introduction

In recent years, development of reactive separation processes as alternatives to conventional processes has been actively pursued. Reaction can be combined with separation techniques such as distillation (DeGarmo et al., 1992; Doherty and Buzad, 1992), crystallization (Berry and Ng, 1997; Mersmann and Kind, 1988), liquid-liquid extraction (Samant and Ng, 1998a; Sharma, 1988), adsorption (Coca et al., 1993; Tonkovich and Carr, 1994), and membrane separation (Tsotsis et al., 1993) to gain certain advantages, such as reduced capital investment and freedom from equilibrium limitations, that cannot be matched by conventional processes.

Extractive reaction processes involve simultaneous reaction and liquid-liquid phase separation. The immiscibility may occur naturally within the reactive system or may be introduced deliberately by adding solvent(s). Many examples of extractive reaction processes are known (for example, Anderson and Veysoglu, 1973; King et al., 1985; Chapman, 1987; Kuntz, 1987; Pahari and Sharma, 1991). The combination of reaction with liquid-liquid phase separation can be utilized effectively to significantly improve yields of desired products, selectivities to desired products in multireaction systems, and separation of byproducts. Extractive reaction processes, however, may not be advantageous in every case and it is highly desirable to formulate a systematic framework for developing potential processes. Toward this goal, a procedure based on equilibrium thermodynamics was developed for synthesis of single- and multistage extractive reaction processes (Samant and Ng, 1998a). Key features of the reactive phase diagrams that are relevant to achieving the above objectives were identified, and the advantages of these processes over conventional single-phase processes were demonstrated with several examples. This framework was extended further to include an efficient and general method for designing an equilibrium-limited multistage extractive reactor (Samant and Ng, 1998b). This procedure was used to evaluate process tradeoffs and to screen process alternatives. However, chemical kinetics and, more importantly, mass transfer may influence the possible benefits obtainable from extractive reactions. The objective of this article is to generalize this framework to account for the interaction between reaction kinetics and mass transfer, as well as their effect on the performance of extractive reaction processes. The focus is not on rigorous modeling, but on obtaining insights for process design. Hence, a generic model introduced here is simple to analyze, but retains the essential features of nonideal thermodynamics and multicomponent mass transfer.

The model equations are developed for a stirred cell that represents a single-stage extractive reactor or any stage of a

Correspondence concerning this article should be addressed to K. M. Ng.

multistage extractive reactor (MSER). Activity-based rate expressions are used to describe reaction kinetics and generalized Maxwell-Stefan formulation are used in conjunction with the film theory is used to describe multicomponent mass transfer. The performance of the stirred cell is shown to be governed by Damköhler number matrices for reaction and mass transfer, as illustrated through several examples. Examples I and II consider systems with inherent phase separation. These examples illustrate the composition loci of the stirred cell in different kinetic regimes of operation, interplay between reaction and mass transfer, enhancement of mass transfer due to reaction, and evaluate the performance of the stirred cell. Examples III and IV consider systems in which phase separation is induced by solvent addition. These examples illustrate the possible benefits such as improvement in yield and selectivity that can be obtained from extractive reaction processes in various operating regimes constrained by reaction, mass transfer, or thermodynamics.

Mathematical Model of a Liquid-Liquid Stirred Cell with Multiple Reactions

Consider a multicomponent system of c components undergoing r chemical reactions. The r reactions can be represented as:

$$\upsilon_{1,m}A_1 + \upsilon_{2,m}A_2 + \ldots + \upsilon_{c,m}A_c = 0 \qquad m = 1, 2, \ldots, r \quad (1)$$

where A_i are the reacting species and $\upsilon_{i,m}$ is the stoichiometric coefficient of component i in reaction m. By convention, $\upsilon_{i,m} < 0$ if component i is a reactant; $\upsilon_{i,m} > 0$ if component i is a product; and $\upsilon_{i,m} = 0$ if it is an inert. Using vector-matrix formalism, we define:

$$\upsilon_i^T = (\upsilon_{i,1}, \upsilon_{i,2}, \ldots, \upsilon_{i,r}) \quad (2)$$

$$\upsilon_{\mathrm{TOT}}^T = (\upsilon_{\mathrm{TOT},1}, \upsilon_{\mathrm{TOT},2}, \ldots, \upsilon_{\mathrm{TOT},r}) \quad (3)$$

where υ_i^T is the row vector of stoichiometric coefficients of component i in each reaction and $\upsilon_{\mathrm{TOT}}^T$ is the row vector of the sum of the stoichiometric coefficients for each reaction.

The stirred cell is a CSTR with two liquid phases separated by a well-defined interface (Figure 1). Feed stream of composition z^F and molar flow rate F and solvent stream of composition z^S and molar flow rate S form the input streams. Extract stream of composition x^E and molar flow rate E and raffinate stream of composition x^R and molar flow rate R are the output streams. In general, we refer to the solvent-rich stream and phase as extract and the solvent-lean stream and phase as raffinate. However, examples with inherent phase separation (no solvent added) are also considered. In these cases, this nomenclature is arbitrary. In the stirred cell, both the extract and raffinate phases are perfectly mixed except for thin stagnant films next to the interface. The resistance to mass transfer in each phase is concentrated in these thin films. Mass transfer through these films takes place in the direction normal to the interface. The r chemical reactions described by Eq. 1 may take place in any one phase or in both phases.

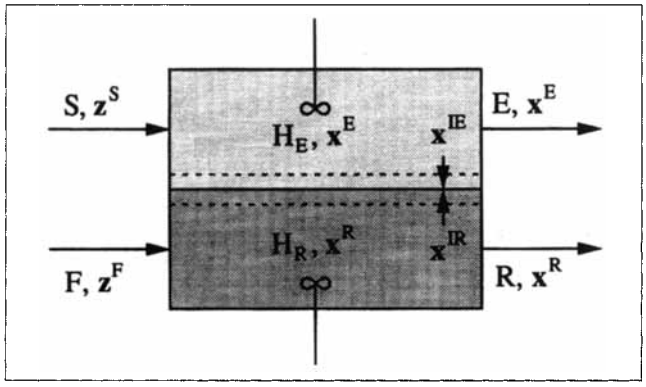

Figure 1. Simple stirred cell.

Reaction kinetics

To describe the reaction kinetics, rate expressions based on mole fractions and activity coefficients, not concentrations, are used. Mole fractions and activity coefficients conform more naturally to the method of writing conservation equations and to the phase and reaction equilibrium models. In addition, this approach gives reaction rate constants with units of reciprocal time regardless of the order of the reaction (Venimadhavan et al., 1994). The rate of reaction i per mole of liquid mixture of composition x is written as:

$$r_i(x) = k_{f_i}\left[\prod_{m=1}^{c_r}(\gamma_m x_m)^{|\upsilon_{m,i}|} - \frac{1}{K_i}\prod_{n=1}^{c_p}(\gamma_n x_n)^{|\upsilon_{n,i}|}\right] \quad (4)$$

where $m = 1, 2, \ldots, c_r$ are the reactants for this reaction, and $n = 1, 2, \ldots, c_p$ are the products of this reaction ($c_r + c_p \le c$). For reaction i, k_{f_i} is the forward reaction rate constant, and K_i is the reaction equilibrium constant:

$$K_i(T) = \frac{k_{f_i}}{k_{r_i}} = \exp\left(\frac{-\Delta G_i}{R_g T}\right) \quad (5)$$

where ΔG_i is the standard Gibbs energy change of reaction i, and R_g is the universal gas constant. Reaction equilibrium occurs at temperatures and compositions which satisfy

$$K_i(T) = \prod_{n=1}^{c}(\gamma_n x_n)_{\mathrm{eq}}^{\upsilon_{n,i}} \quad (6)$$

where the subscript eq indicates reaction equilibrium.

Mass transfer

Description of mass transfer in the stirred cell is based on the generalized suitable Maxwell-Stefan formulation. It is the approach most generally used for describing mass transfer in multicomponent systems and it takes proper account of thermodynamic nonidealities. For transfer within the stirred cell, Maxwell-Stefan diffusion equations need to be solved along with the equation of continuity for each phase:

$$\bar{\nabla}\cdot\bar{N}_i^{\phi} = Y\upsilon_i^T\mathcal{R}(x^{\phi}) \qquad i = 1, 2, \ldots, c; \quad \phi = R, E \quad (7)$$

and the condition of phase equilibrium at the interface:

$$\gamma_i^{IR}x_i^{IR} = \gamma_i^{IE}x_i^{IE} \qquad i = 1, 2, \ldots, c \quad (8)$$

Overbars indicate directional quantities, and superscript I indicates quantities evaluated at the interface. $\mathfrak{R}(x)$ is the column vector of reaction rates evaluated at composition x, and $\bar{N}_i^{\phi}$ represents the molar flux relative to stationary coordinates in phase ϕ. The binary integer parameter Y equals unity if the phase is reactive and zero if the phase is nonreactive. Solutions to Eq. 7 for $Y=0$, in combination with Eq. 8, are available for various hydrodynamic models, such as the film model (Krishna and Standart, 1976; Krishna, 1977) and the penetration model (Krishna, 1978). For $Y=1$, numerical solutions with some simplifying assumptions are also available (Sentarli and Hortacsu, 1987; Frank et al., 1995).

Along the lines of Krishna and Wesselingh (1997), the molar transfer fluxes at the interface can be written in terms of mass-transfer coefficients ($K_{m_{ij}}^{I\phi}, \phi = R, E$) as:

$$\bar{N}_i^{I\phi} = \bar{J}_i^{I\phi} + x_i^{I\phi}\bar{N}_T^{I\phi} = -c_T^{\phi}K_{m_{ij}}^{I\phi}\Delta x_j^{\phi} + x_i^{I\phi}\bar{N}_T^{I\phi} \qquad i=1, 2, \ldots, c-1; \quad \phi = R, E$$

$$\bar{N}_c^{I\phi} = \bar{N}_T^{I\phi} - \sum_{k=1}^{c-1}\bar{N}_k^{I\phi} \qquad \phi = R, E \tag{9}$$

Here (and in the rest of this section), repeated indices imply summation. The composition difference driving forces are defined as:

$$\Delta x_i^R = x_i^{IR} - x_i^R \qquad i=1, 2, \ldots, c-1$$
$$\Delta x_i^E = x_i^E - x_i^{IE} \qquad i=1, 2, \ldots, c-1 \tag{10}$$

x_i^R and x_i^E are the bulk raffinate and extract phase mole fractions. Although the concentration-driving forces are directional quantities, they are not marked with overbars, since the sense of direction is preserved in these definitions. By comparison with Maxwell-Stefan diffusion equations (Taylor and Krishna, 1993), the mass-transfer coefficients ($K_{m_{ij}}^{I\phi}, \phi = R, E$) can be written as:

$$K_{m_{ij}} = B_{ik}^{-1}\Gamma_{kj} \qquad i, j = 1, 2, \ldots, c-1 \tag{11}$$

where

$$B_{ii} = \frac{x_i}{\kappa_{ic}} + \sum_{\substack{k=1\\k\neq i}}^{c}\frac{x_k}{\kappa_{ik}}, \quad B_{ij(i\neq j)} = -x_i\left(\frac{1}{\kappa_{ij}} - \frac{1}{\kappa_{ic}}\right) \qquad i, j = 1, 2, \ldots, c-1 \tag{12}$$

$$\Gamma_{ij} = \delta_{ij} + x_i\frac{\partial \ln \gamma_i}{\partial x_j}, \quad \delta_{ii} = 1, \quad \delta_{ij(i\neq j)} = 0 \qquad i, j = 1, 2, \ldots, c-1 \tag{13}$$

Here, superscripts I, R, and E are omitted for convenience. κ_{ij} represents the mass-transfer coefficients of the binary pairs in the multicomponent mixture. These coefficients can be measured experimentally or estimated using correlations in standard texts such as Sherwood et al. (1975) and King (1980).

Writing the molar fluxes at the interface in this form provides two major advantages. The influence of all binary pair diffusivities is retained, and the solution to the one-dimensional continuity equation (Eq. 7) can be written as a simple algebraic equation, thus eliminating the need for extensive computations. A drawback of this representation is that although the mass-transfer coefficients at the interface are assumed to be constant, they depend slightly on forward reaction rates and, to a greater extent, on composition. However, Maxwell-Stefan diffusivities for realistic extractive reaction systems are difficult to estimate and expected to have a large degree of uncertainty associated with them. Extensive experimental data for a given system are typically required to estimate either the diffusivities or the mass-transfer parameters. Therefore, the use of mass transfer coefficients as defined above is a convenient and practical approach.

Bootstrap solution

The description of mass transfer given by Eqs. 8 to 10 is not complete as these equations are not closed (i.e., we need to know $\bar{N}_T^{I\phi}$ to evaluate $\bar{N}_c^{I\phi}$ and $\bar{N}_c^{I\phi}$ to evaluate $\bar{N}_T^{I\phi}$). This closure problem is known as the Bootstrap problem (Krishna and Taylor, 1986) and is resolved here by using the continuity of molar fluxes at the interface. At the interface, the continuity of fluxes implies

$$\bar{N}_i^{IR} = \bar{N}_i^{IE} = \bar{N}_i^{I} \qquad i=1, 2, \ldots, c-1$$
$$\bar{N}_T^{IR} = \bar{N}_T^{IE} = \bar{N}_T^{I} \tag{14}$$

After some algebraic manipulation of Eqs. 9 and 14, we can write

$$\bar{N}_T^I(x_i^{IR} - x_i^{IE}) = \left(c_T^R K_{m_{ij}}^{IR}\Delta x_j^R - c_T^E K_{m_{ij}}^{IE}\Delta x_j^E\right) \qquad i=1, 2, \ldots, c-1 \tag{15}$$

Using Eqs. 9 and 15, we can write

$$\bar{N}_i^I = c_T^E\beta_{ik}^E K_{m_{kj}}^{IE}\Delta x_j^E + c_T^R\beta_{ik}^R K_{m_{kj}}^{IR}\Delta x_j^R \qquad i=1, 2, \ldots, c-1$$
$$\bar{N}_c^I(x_i^{IR} - x_i^{IE}) = \left(c_T^R K_{m_{ij}}^{IR}\Delta x_j^R - c_T^E K_{m_{ij}}^{IE}\Delta x_j^E\right) - (x_i^{IR} - x_i^{IE})\sum_{k=1}^{c-1}\bar{N}_k^I \qquad i=1, 2, \ldots, c-1 \tag{16}$$

where the diagonal matrices β^E and β^R are given by

$$\beta_{kk}^E = x_k^{IR}/(x_k^{IE} - x_k^{IR}), \qquad \beta_{jk(j\neq k)}^E = 0 \qquad j, k = 1, 2, \ldots, c-1$$
$$\beta_{kk}^R = x_k^{IE}/(x_k^{IR} - x_k^{IE}), \qquad \beta_{jk(j\neq k)}^R = 0 \qquad j, k = 1, 2, \ldots, c-1 \tag{17}$$

Equation 16, with Eqs. 8 and 10, completely describes the mass transfer across the interface of the stirred cell.

Conservation equations

The overall and component material balance equations for the stirred cell can be written as

$$R = F + YH_R v^T_{\mathrm{TOT},m} r_m(\boldsymbol{x}^R) - a\bar{N}^I_T \tag{18}$$

$$Rx^R_i = Fz^F_i + YH_R v^T_{i,m} r_m(\boldsymbol{x}^R) - a\bar{N}^I_i \qquad i = 1, 2, \ldots, c-1 \tag{19}$$

$$E = S + YH_E v^T_{\mathrm{TOT},m} r_m(\boldsymbol{x}^E) + a\bar{N}^I_T \tag{20}$$

$$Ex^E_i = Sz^S_i + YH_E v^T_{i,m} r_m(\boldsymbol{x}^E) + a\bar{N}^I_i \qquad i = 1, 2, \ldots, c-1 \tag{21}$$

In writing these equations, the molar holdups in the films in each phase were assumed to be negligible in comparison to the total molar holdup in the bulk of each phase. Hence, the compositions of the extract and the raffinate streams are the same as the bulk compositions of the extract and the raffinate phases, respectively. This assumption is generally valid for all types of industrial liquid-liquid contactors (Krishna and Sie, 1994). Dividing Eqs. 18 to 21 by $(F+S)$ and using the constitutive equations for reaction kinetics and mass transfer (Eqs. 4, 15, and 16), we get

$$\frac{R}{(F+S)} = \frac{F}{(F+S)} + v^T_{\mathrm{TOT},m} Da^R_{r_{mp}} k^{-1}_{f_{pq}} r_q(\boldsymbol{x}^R) + \left[\frac{Da^E_{m_{kj}}\left(x^E_j - x^{IE}_j\right) - Da^R_{m_{kj}}\left(x^{IR}_j - x^R_j\right)}{\left(x^{IR}_k - x^{IE}_k\right)}\right] \tag{22}$$

$$\frac{R}{(F+S)} x^R_i = \frac{F}{(F+S)} z^F_i + v^T_{i,m} Da^R_{r_{mp}} k^{-1}_{f_{pq}} r_q(\boldsymbol{x}^R) - \beta^R_{ik} Da^R_{m_{kj}}\left(x^{IR}_j - x^R_j\right) - \beta^E_{ik} Da^E_{m_{kj}}\left(x^E_j - x^{IE}_j\right) \qquad i = 1, 2, \ldots, c-1 \tag{23}$$

$$\frac{E}{(F+S)} = \frac{S}{(F+S)} + v^T_{\mathrm{TOT},m} Da^E_{r_{mp}} k^{-1}_{f_{pq}} r_q(\boldsymbol{x}^E) - \left[\frac{Da^E_{m_{kj}}\left(x^E_j - x^{IE}_j\right) - Da^R_{m_{kj}}\left(x^{IR}_j - x^R_j\right)}{\left(x^{IR}_k - x^{IE}_k\right)}\right] \tag{24}$$

$$\frac{E}{(F+S)} x^E_i = \frac{S}{(F+S)} z^S_i + v^T_{i,m} Da^E_{r_{mp}} k^{-1}_{f_{pq}} r_q(\boldsymbol{x}^E) + \beta^R_{ik} Da^R_{m_{kj}}\left(x^{IR}_j - x^R_j\right) + \beta^E_{ik} Da^E_{m_{kj}}\left(x^E_j - x^{IE}_j\right) \qquad i = 1, 2, \ldots, c-1 \tag{25}$$

where $\boldsymbol{k}_f$ is the diagonal matrix of forward reaction rate constants:

$$k_{f_{qq}} = k_{f_q}, \qquad k_{f_{pq(p\neq q)}} = 0 \qquad p, q = 1, 2, \ldots, r \tag{26}$$

and the dimensionless Damköhler number matrices for reaction $(\boldsymbol{Da}^R_r, \boldsymbol{Da}^E_r)$ and mass transfer $(\boldsymbol{Da}^R_m, \boldsymbol{Da}^E_m)$ are defined as

$$Da^\phi_{r_{pp}} = Y\frac{H_\phi/(F+S)}{1/k_{f_p}}, \qquad Da^\phi_{r_{pq(p\neq q)}} = 0 \qquad p, q = 1, 2, \ldots, r; \quad \phi = R, E \tag{27}$$

$$Da^\phi_{m_{ij}} = \frac{H_\phi/(F+S)}{H_\phi/ac^\phi_T K^{I\phi}_{m_{ij}}}, \qquad i, j = 1, 2, \ldots, c-1; \quad \phi = R, E \tag{28}$$

Note that in Eqs. 22 and 24, $\bar{N}^I_T$ is evaluated by using a particular component index $k \in \{1, 2, \ldots, c-1\}$. We could have equivalently used any other component index $(\neq k)$. Hence, for a particular choice of k, we have $(c-2)$ additional equations given by

$$\left[\frac{Da^E_{m_{kj}}\left(x^E_j - x^{IE}_j\right) - Da^R_{m_{kj}}\left(x^{IR}_j - x^R_j\right)}{\left(x^{IR}_k - x^{IE}_k\right)}\right] = \left[\frac{Da^E_{m_{ij}}\left(x^E_j - x^{IE}_j\right) - Da^R_{m_{ij}}\left(x^{IR}_j - x^R_j\right)}{\left(x^{IR}_i - x^{IE}_i\right)}\right] \tag{29}$$

$$k \in \{1, 2, \ldots, c-1\}; \qquad i = 1, 2, \ldots, c-1; \qquad i \neq k$$

In addition, the mole fractions of inlet streams, mole fractions in the bulk phases, and the mole fractions at the interface add up to unity:

$$\sum_{i=1}^{c} z^F_i = \sum_{i=1}^{c} z^S_i = \sum_{i=1}^{c} x^R_i = \sum_{i=1}^{c} x^E_i = \sum_{i=1}^{c} x^{IR}_i = \sum_{i=1}^{c} x^{IE}_i = 1.0 \tag{30}$$

Equations 22 to 25 along with Eqs. 8, 29 and 30 complete the general mathematical model for the stirred cell. In these equations the effects of reaction kinetics and mass transfer are parametrized by the dimensionless Damköhler number matrices for reaction $(\boldsymbol{Da}^R_r, \boldsymbol{Da}^E_r)$ and mass transfer $(\boldsymbol{Da}^R_m, \boldsymbol{Da}^E_m)$ which are defined above.

The Damköhler numbers for reaction are the conventional first Damköhler numbers. The definition of Damköhler numbers for mass transfer is unconventional, but is useful for an open system. The Damköhler numbers for reaction and mass transfer compare the characteristic residence time of a phase to the characteristic time for reaction and mass transfer, respectively, in that phase. Typically, in thermodynamically nonideal systems, the flux of a component is governed not only by its own composition gradient but also by the composition gradients of other components in the reacting mixture. Hence, the Damköhler number matrices for mass transfer, $\boldsymbol{Da}^R_m$ and $\boldsymbol{Da}^E_m$, are not necessarily diagonal and the effect of the off-diagonal elements on the performance of the stirred cell can be quite significant. The model equations allow us to easily account for the effects of the off-diagonal elements of $\boldsymbol{Da}^R_m$ and $\boldsymbol{Da}^E_m$.

Degrees of freedom

The number of independent variables is determined for the stirred cell model. The material balance equations (Eqs. 22

to 25) represent a set of $(2c)$ equations. In addition, we have (c) equations given by Eq. 8, $(c-2)$ constraints given by Eq. 29, and six equations given by Eq. 30. Hence, the model equations form a set of $(4c+4)$ equations, which contain the following $(6c+4)$ variables: F, S, E, R, z^F, z^S, x^E, x^R, x^{IE}, and x^{IR}. We have $(2c)$ degrees of freedom, which are specified by fixing F, S, z_i^F $(i=1, 2, \ldots, c-1)$, and z_i^S $(i=1, 2, \ldots, c-1)$. Thus, for given molar flow rates and compositions of the feed and the solvent streams to the stirred cell, the interplay between chemical kinetics and mass transfer and their effect on extractive reactions can be completely described in terms of the Damköhler number matrices.

Systems with Inherent Phase Separation

Liquid-liquid reactions often involve systems in which reactants exist in different phases and the reactions take place in one of the phases. Hence, the analysis will be started with two examples where the reactants are partially miscible with each other.

Example I: Three-Component System with One Reaction

Let us consider a three-component system with the following reaction:

$$A + B \Leftrightarrow C \tag{31}$$

where components A and B are partially miscible, but the product C is completely miscible with both. The reaction rate per mole of liquid mixture of composition x is given by

$$r(x) = k_f\left(\gamma_A x_A \gamma_B x_B - \frac{\gamma_C x_C}{K}\right) \tag{32}$$

Thermodynamic parameters for this system (Sorenson and Arlt, 1979) are listed in Table 1 and the phase diagram is shown in Figure 2. Curve *apb* is the phase envelope and curve *AREB* is the reaction equilibrium curve. The dashes represent the tie-lines and the arrows represent the stoichiometric lines. The phase and reaction equilibrium curves intersect at points R and E; the two end-points of the unique reactive tie-line RE. The shaded region, bounded by the stoichiometric lines through points R and E, represents the two-phase region. If the overall initial composition of the system lies in this region, the system would split into two phases with compositions corresponding to points R and E at phase and reaction equilibrium. Thus, the end-points R and E of the reactive tie-line represent the equilibrium thermodynamic limits for this system in the two-phase region.

Table 1. Thermodynamic Parameters for Example I

Temp. = 313.15 K; Pres. = 1 atm; Equil. Const., $K = 0.035$		
UNIQUAC Equation Parameters (Sorenson and Arlt, 1979)		
Pure Component Parameters		
Component	r	q
A (1)	4.0464	3.240
B (3)	2.7384	2.472
C (2)	3.1878	2.400
Binary Interaction Parameters (K)		
$a(1,1) = 0.0$	$a(1,2) = -68.716$	$a(1,3) = 257.56$
$a(2,1) = -89.186$	$a(2,2) = 0.0$	$a(2,3) = -155.49$
$a(3,1) = 122.36$	$a(3,2) = 66.225$	$a(3,3) = 0.0$

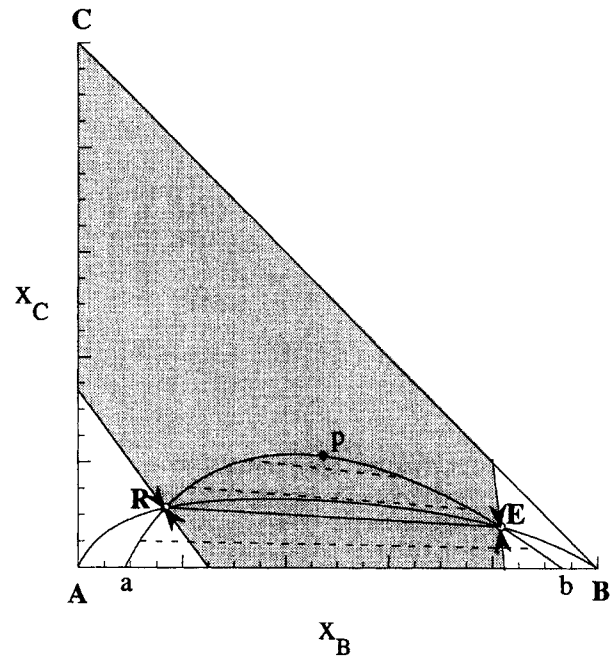

Figure 2. Phase diagram for Example I ($K = 0.035$).

Consider the stirred cell with input streams of pure A $(z_A^F = 1.0,\ F = 1.0)$ and pure B $(z_B^S = 1.0,\ S = 1.0)$. We refer to the A-rich phase as the raffinate phase and the B-rich phase as the extract phase. As can be seen from Eqs. 22 to 25, the performance of the stirred cell can be characterized by the following parameters:

$$\mathbf{Da}_r^{\phi} = [Da_r^{\phi}], \quad \mathbf{Da}_m^{\phi} = \begin{bmatrix} Da_{m_{AA}}^{\phi} & Da_{m_{AB}}^{\phi} \\ Da_{m_{BA}}^{\phi} & Da_{m_{BB}}^{\phi} \end{bmatrix}, \quad \phi = R, E \tag{33}$$

Without loss of generality, in this and the following examples, let us assume that the reaction takes place in the raffinate phase only $(\mathbf{Da}_r^E = 0)$. We will now investigate the influence of these parameters on the operation of the stirred cell.

Composition loci for the stirred cell

The stirred-cell loci in the raffinate and the extract phase represent the steady-state compositions of these phases for various values of the Damköhler numbers. Let us start by assuming that the molar flux of each component is governed by its own composition gradient (diagonal $\mathbf{Da}_m^R$ and $\mathbf{Da}_m^E$) and that the mass-transfer coefficients of all components are the same $(Da_{m_{AA}}^{\phi} = Da_{m_{BB}}^{\phi} = Da_m^{\phi}, \phi = R, E)$. Figures 3a and 3b, which correspond to the enlarged left and right corner regions of the phase diagram in Figure 2, show the stirred-cell loci, for a low value (unity) of Da_m^E, in the raffinate and the extract phase, respectively. In Figure 3a the raffinate phase loci are plotted as a function of increasing Da_r^R for fixed values of Da_m^R ranging from 0.1 to 100. For $Da_r^R = 0$, no C is

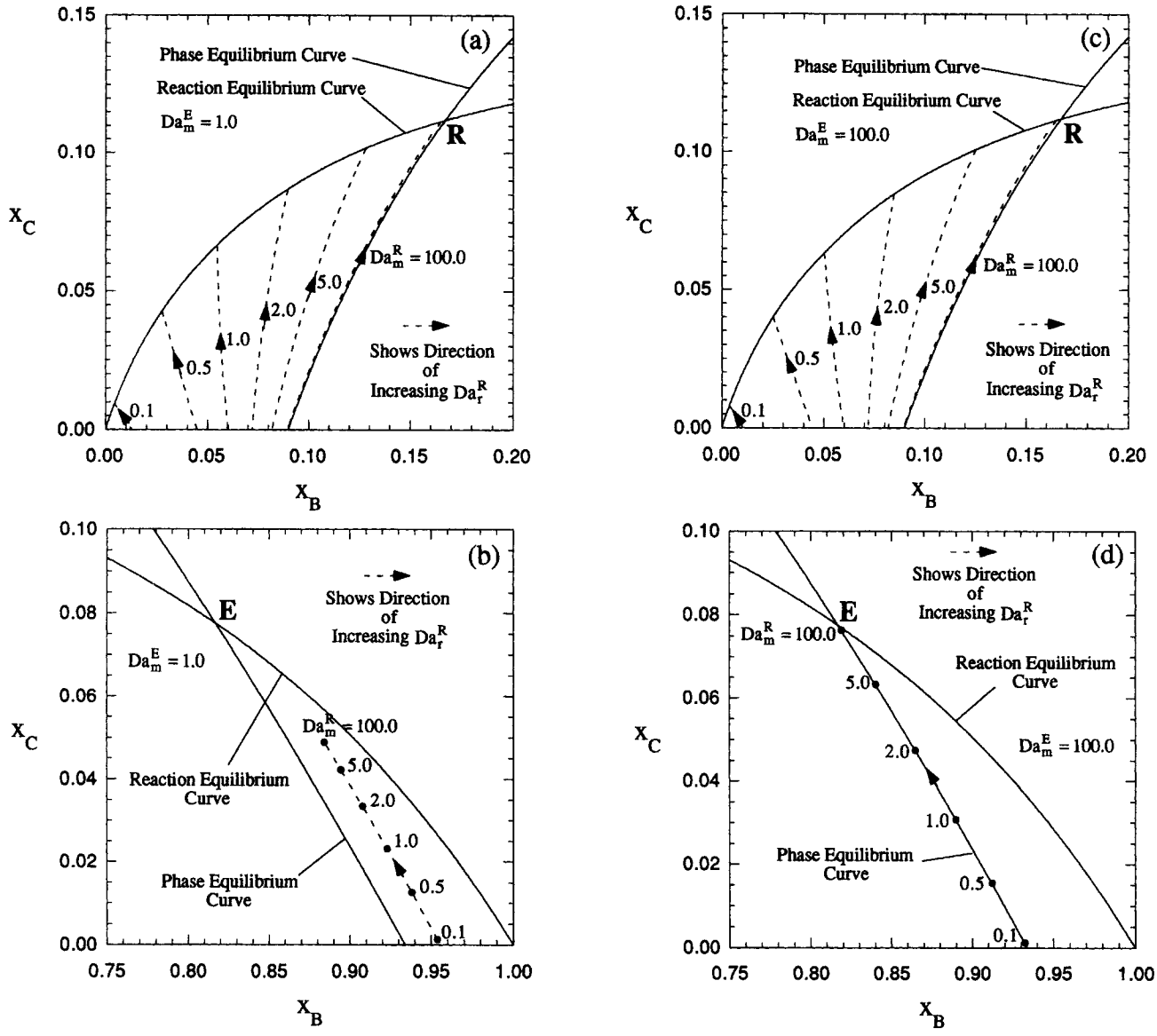

Figure 3. Composition loci for the stirred cell.

(a) Raffinate phase loci for $Da_m^E = 1.0$; (b) extract phase loci for $Da_m^E = 1.0$; (c) raffinate phase loci for $Da_m^E = 100.0$; (d) extract phase loci for $Da_m^E = 100.0$.

formed and the raffinate phase composition lies on the A-B edge (abscissa). For low values of Da_r^R, the composition of the raffinate phase is still far from the reaction equilibrium curve, since the residence time of the raffinate phase is much shorter than the characteristic reaction time. At very high values of Da_r^R, the residence time is sufficiently longer than the characteristic reaction time and the raffinate composition lies close to the reaction equilibrium curve. We also observe that as Da_m^R increases from 0.1 to 100, the loci move toward the phase equilibrium curve. At low values of Da_m^R, the residence time of the raffinate phase is much shorter than the characteristic time for mass transfer of A and B, and therefore the bulk composition is far from the phase equilibrium curve. As these Damköhler numbers increase, however, the residence time increases in comparison to the characteristic mass transfer time, and the bulk raffinate composition approaches the interface composition which lies on the phase equilibrium curve. In the limit of high Da_r^R and Da_m^R, the raffinate composition tends to point R which lies on both phase and reaction equilibrium curves (thermodynamic limit for raffinate).

Figure 3b shows that the extract phase loci lie on a single curve. The extract composition is always far from the phase equilibrium curve, since Da_m^E (unity) is low. As Da_r^R increases for fixed values of Da_m^R, the extract loci do not tend to the reaction equilibrium curve as the reaction takes place only in the raffinate phase. Instead, the loci approach the limits shown by filled circles corresponding to the curves in Figure 3a. For high values of Da_r^R and Da_m^R, the extract composition does not reach the thermodynamic limit (point E).

Now let us consider the case where the resistance to mass transfer in the extract phase is negligible. Figures 3c and 3d show the stirred-cell loci, for a high value (100) of Da_m^E, in the raffinate and the extract phase, respectively. The raffi-

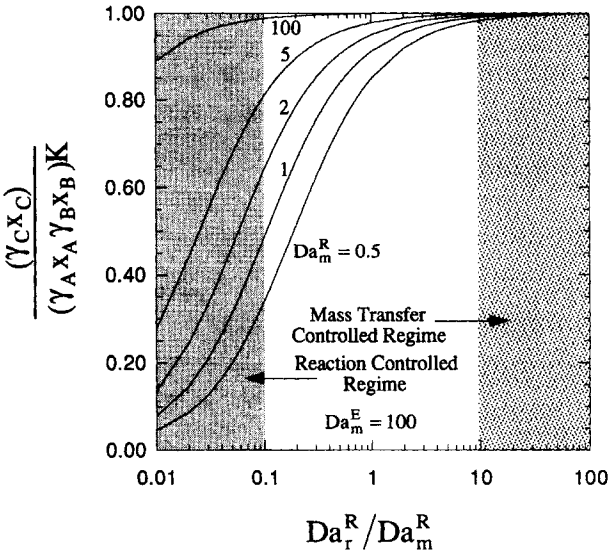

Figure 4. Departure of the bulk raffinate composition from reaction equilibrium.

nate-phase loci show the same behavior as Figure 3a, while the extract compositions always lie extremely close to the phase equilibrium curve. Also, in the limit of high Da_r^R and Da_m^R, the extract composition now tends to the thermodynamic limit (point E).

Interplay of reaction and mass transfer

Rates of reaction and mass transfer relative to the rate of product removal govern the composition loci of the stirred cell. In addition, useful insights regarding the interplay of reaction and mass transfer can be obtained from their rates relative to each other. Figure 4 shows the departure from reaction equilibrium (expressed as the ratio of the reaction equilibrium constant calculated using actual mole fractions to the thermodynamic value) of the bulk raffinate composition as a function of Da_r^R/Da_m^R. It was assumed that $\boldsymbol{Da}_m^R$ and $\boldsymbol{Da}_m^E$ are diagonal, the mass-transfer coefficients of all components are the same ($Da_{m_{AA}}^{\phi} = Da_{m_{BB}}^{\phi} = Da_m^{\phi}, \phi = R, E$), and Da_m^E is high (100). The ratio of the Damköhler numbers (Da_r^R/Da_m^R) is the conventional second Damköhler number and is, in principle, similar to the Hatta number or Thiele modulus:

$$\frac{Da_r^R}{Da_m^R} = \frac{\text{Characteristic Mass Transfer Time}}{\text{Characteristic Reaction Time}} \; (\equiv Ha^2 \text{ or } \Phi^2) \tag{34}$$

High values of Da_r^R/Da_m^R represent the mass-transfer-controlled regime, in which the reaction is much faster than mass transfer across the interface. The reaction takes place essentially in the film near the interface, and the bulk is in reaction equilibrium. Low values of Da_r^R/Da_m^R represent the reaction-controlled regime. In this regime, the reaction is much slower than mass transfer. Because the reaction takes place both in the film and in the bulk, the bulk composition shows significant departure from reaction equilibrium. The reaction-controlled and mass-transfer-controlled regimes are indicated in Figure 4 by the light and dark shaded regions, respectively (the same convention is followed for other examples). It should be noted that the boundaries of these regimes are not sharp.

Recall that the composition loci and the performance of the stirred cell depend not only on the relative rates of reaction and mass transfer but also on their rates relative to the rate of product removal. Therefore, the departure from reaction equilibrium becomes more pronounced, especially in the reaction-controlled regime, as the value of Da_m^R decreases from 100 to 0.5 (i.e., when both reaction and mass transfer are much slower compared to product removal).

Enhancement of mass transfer

The presence of reaction in the raffinate phase enhances the transfer of A and B across the interface. This can be quantified by the enhancement factor which is the ratio of the molar flux across the interface with reaction to that without reaction:

$$E_{i\,|\,Da_r^R} = \frac{\overline{N}_{i\,|\,Da_r^R}^I}{\overline{N}_{i\,|\,Da_r^R=0}^I} \qquad i = A, B \tag{35}$$

The enhancement factors for A and B are shown in Figures 5a and 5b, respectively, for the cases considered in Figure 4. As we go from the reaction-controlled regime (low Da_r^R/Da_m^R) to the mass-transfer-controlled regime (high Da_r^R/Da_m^R), the enhancement factors increase from unity (for $Da_r^R = 0$) to their equilibrium values. These equilibrium values are reached in the mass-transfer-controlled regime where the bulk raffinate phase is in reaction equilibrium (Figure 4). Hence, any further increase in Da_r^R/Da_m^R does not result in further enhancement of mass transfer. The enhancement of mass transfer becomes increasingly significant as the residence time increases in comparison to the characteristic times for reaction and mass transfer (i.e., as Da_m^R increases).

Effect of off-diagonal terms on conversion

In this example, the conversion of A can be improved by facilitating transport of B into the raffinate phase and by inhibiting transport of A out of the raffinate phase. Figures 6a and 6b show the dependence on Da_r^R of the effective dimensionless resistances to the transport of A and B across the interface for various values of $\boldsymbol{Da}_m^R$. $\boldsymbol{Da}_m^E$ is assumed to be diagonal ($Da_{m_{AA}}^E = Da_{m_{BB}}^E = Da_m^E = 100$). The dimensionless resistance to mass transfer is defined as

$$\frac{(F+S)\Delta x_i^R}{-a\overline{N}_i^I} \qquad i = A, B \tag{36}$$

Note that the quantity in Eq. 36 is always positive as Δx_i^R and $\overline{N}_i^I$ ($i = A, B$) have opposite signs. An increase in $Da_{m_{BB}}^R$ from 5 to 20 reduces the resistance to mass transfer of B (curves a and b, Figure 6b); a decrease in $Da_{m_{AA}}^R$ from 5 to 2 increases the resistance to mass transfer of A (curves b and c, Figure 6a). As Δx_A^R is negative, negative values of $Da_{m_{BA}}^R$ further reduce the resistance to mass transfer of B (curves c

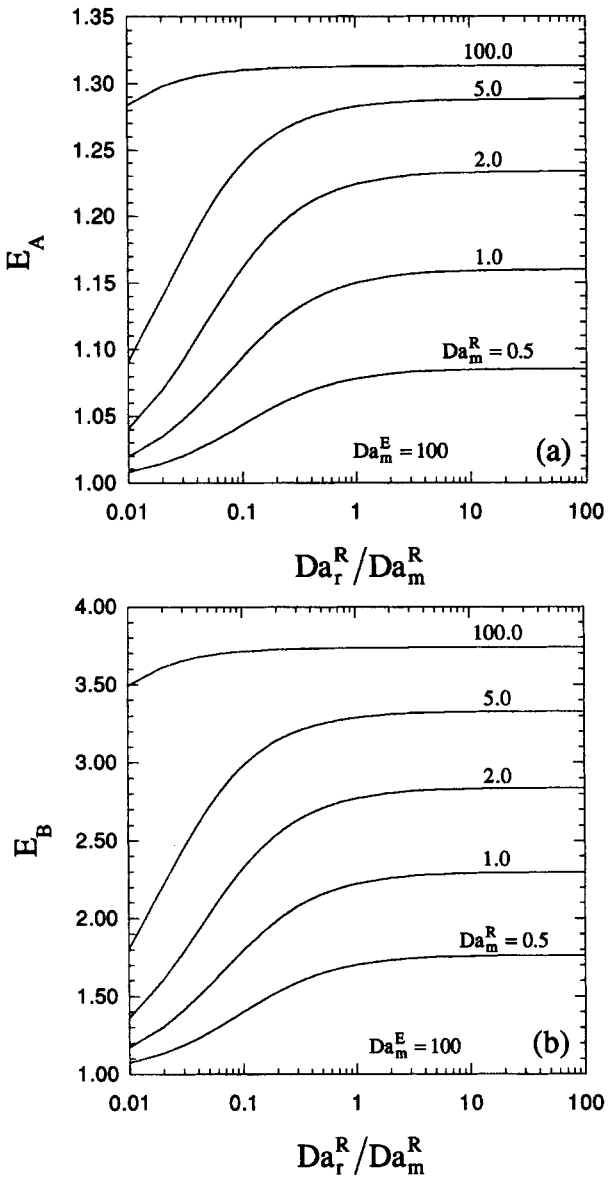

Figure 5. Enhancement of mass transfer: (a) of *A*; (b) of *B*.

and d, Figure 6b); as Δx_B^R is positive, positive values of $Da_{m_{AB}}^R$ further increase the resistance to mass transfer of A (curves d and e, Figure 6a). Negative values of $Da_{m_{AB}}^R$ decrease the resistance to the transfer of A (curves e and f, Figure 6a). In Figure 6c, conversion of A is plotted as a function of Da_r^R for various values of Da_m^R corresponding to curves a, b, c, d, e and f. Conversion of A increases as we go from curves a, b, f, c, and d, to e in that order, due to the way in which the Damköhler numbers for mass transfer influence the transfer of A and B across the interface, as discussed earlier.

Example II: Four-Component System with Two Reactions

Consider a reactive system comprising components A, B, C, and D with the following reactions:

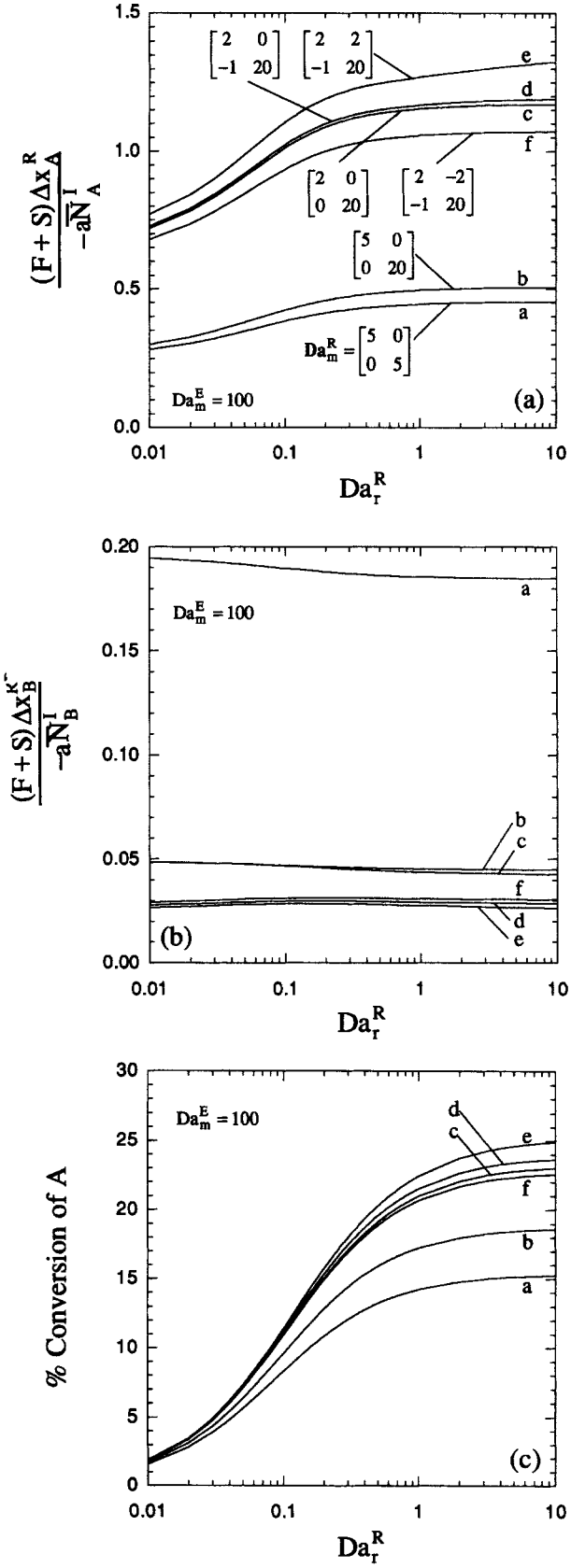

Figure 6. Performance of stirred cell.

(a) Dimensionless resistance to mass transfer of A; (b) dimensionless resistance to mass transfer of B; (c) conversion of A.

$$A + B \Leftrightarrow C$$
$$B + C \Leftrightarrow D \tag{37}$$

Reactants A and B are partially miscible with each other and completely miscible with C and D. C is the desired product, and D is the undesired byproduct. We refer to the first reaction as the desired reaction and the second reaction as the undesired reaction. The rates of the two reactions per mole of liquid mixture of composition $\boldsymbol{x}$ are given by

$$r_1(\boldsymbol{x}) = k_{f_1}\left(\gamma_A x_A \gamma_B x_B - \frac{\gamma_C x_C}{K_1}\right),$$
$$r_2(\boldsymbol{x}) = k_{f_2}\left(\gamma_B x_B \gamma_C x_C - \frac{\gamma_D x_D}{K_2}\right) \tag{38}$$

Phase diagrams for multicomponent multireaction systems at phase and reaction equilibrium can be easily represented using transformed mole fraction coordinates (Ung and Doherty, 1995; Samant and Ng, 1998a). The transformed mole fractions and the transformed phase diagram for this system are shown in Figure 7. The thermodynamic parameters used to generate this diagram are listed in Table 2. According to the Gibbs phase rule, the system has, at constant temperature and pressure, 4(components)-2(reactions)-1(phase) = 1 degree of freedom in the single-phase region and 4(components)-2(reactions)-2(phases) = 0 degrees of freedom in the two-phase region. Hence, the transformed phase diagram is a line, as shown in Figure 7. The two-phase region is shown by the thick line bounded by points R and E. If the overall initial composition of the system lies in this region, at equilibrium the system would split into two phases with compositions corresponding to points R and E. Thus, points R and E represent the equilibrium thermodynamic limits for this system.

Let us consider the stirred cell with input streams of pure A ($z_A^F = 1.0$, $F = 1.5$) and pure B ($z_B^S = 1.0$, $S = 1$). We refer to the A-rich phase as the raffinate phase and the B-rich phase as the extract phase. The performance of the stirred cell is influenced by:

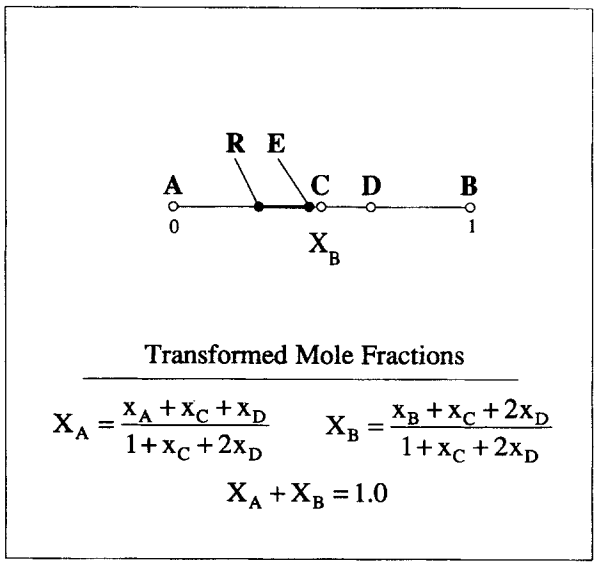

Figure 7. Transformed coordinates and transformed phase diagram for Example II.

Table 2. Thermodynamic Parameters for Example II

Temp. = 298.15 K; Pres. = 1 atm; Equil. Const., $K_1 = 0.7$, $K_2 = 1.3$			
UNIQUAC Equation Parameters (Sorenson and Arlt, 1979)			
Pure Component Parameters			
Component	r	q	
A (1)	3.1878	2.4	
B (2)	2.4088	2.248	
C (3)	2.2024	2.072	
D (4)	3.4543	3.052	
Binary Interaction Parameters (K)			
a (1,1) = 0.0	a (1,2) = 649.05	a (1,3) = 41.146	a (1,4) = 154.55
a (2,1) = 113.53	a (2,2) = 0.0	a (2,3) = 121.11	a (2,4) = 7.4068
a (3,1) = 56.488	a (3,2) = −229.71	a (3,3) = 0.0	a (3,4) = −277.29
a (4,1) = 17.119	a (4,2) = −25.154	a (4,3) = 157.6	a (4,4) = 0.0

$$\boldsymbol{Da}_r^{\phi} = \begin{bmatrix} Da_{r_{11}}^{\phi} & 0.0 \\ 0.0 & Da_{r_{22}}^{\phi} \end{bmatrix},$$
$$\boldsymbol{Da}_m^{\phi} = \begin{bmatrix} Da_{m_{AA}}^{\phi} & Da_{m_{AB}}^{\phi} & Da_{m_{AC}}^{\phi} \\ Da_{m_{BA}}^{\phi} & Da_{m_{BB}}^{\phi} & Da_{m_{BC}}^{\phi} \\ Da_{m_{CA}}^{\phi} & Da_{m_{CB}}^{\phi} & Da_{m_{CC}}^{\phi} \end{bmatrix}, \quad \phi = R, E \tag{39}$$

The performance parameters of interest are the conversion of A and selectivity to the desired product C. These parameters are defined as

$$\text{Conversion of } A = \frac{\text{Amount of } A \text{ Reacted}}{\text{Amount of } A \text{ Fed}}$$
$$\text{Selectivity to } C = \frac{\text{Amount of } C \text{ Produced}}{\text{Amount of } A \text{ Reacted}} \tag{40}$$

At the equilibrium thermodynamic limit, for the given feed and solvent compositions and flow rates, the conversion of A is 40.44% and the selectivity to C is 0.7171.

Trade-off between conversion and selectivity

Let us consider a case where the forward reaction rate constants for both reactions are the same ($Da_{r_{11}}^R = Da_{r_{22}}^R = Da_r^R$), $\boldsymbol{Da}_m^R$ and $\boldsymbol{Da}_m^E$ are diagonal, and mass-transfer coefficients for all components are the same ($Da_{m_{AA}}^{\phi} = Da_{m_{BB}}^{\phi} = Da_{m_{CC}}^{\phi} = Da_m^{\phi}$, $\phi = R, E$). Figure 8a shows the trade-off between conversion of A and selectivity to the desired product C, and Figure 8b shows the departure of the bulk raffinate composition from reaction equilibrium compositions corresponding to the desired and undesired reactions. These figures are plotted as a function of the ratio Da_r^R/Da_m^R for various values of Da_m^R. Da_m^E is fixed at 100. The mass-transfer and reaction-controlled regimes are shown by the dark- and light-shaded regions.

In the reaction controlled regime, bulk raffinate compositions show substantial departure from reaction equilibrium for both reactions. As we go from the reaction-controlled

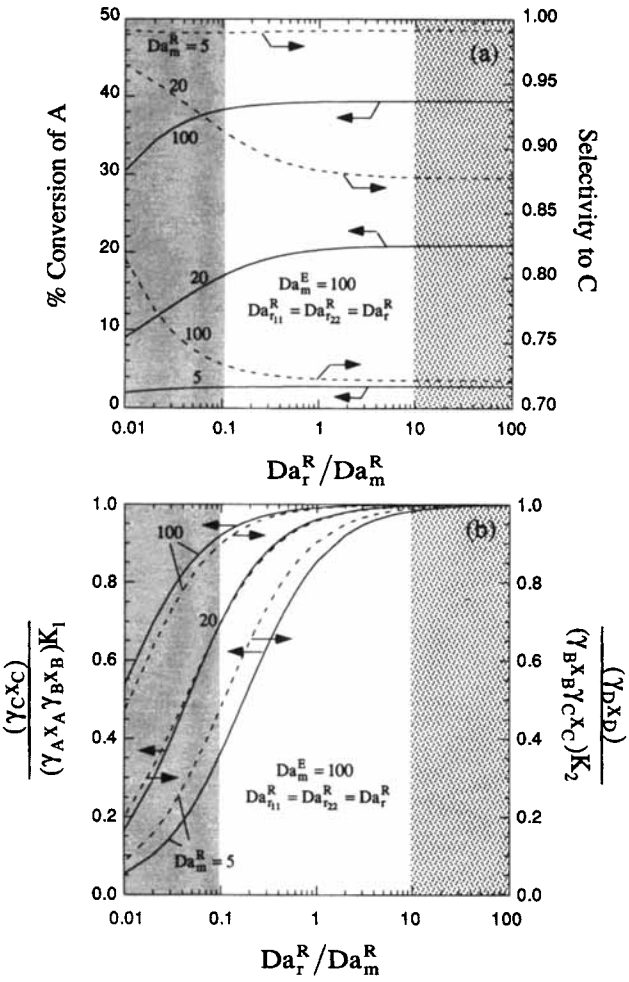

Figure 8. (a) Performance of the stirred cell; (b) departure of the bulk raffinate composition from reaction equilibrium.

regime to the mass-transfer-controlled regime, conversion of A increases from zero (for $Da_r^R = 0$) and the selectivity to C decreases from unity (for $Da_r^R = 0$) to equilibrium values. These equilibrium values are reached in the mass-transfer-controlled regime where the bulk raffinate phase is in reaction equilibrium (Figure 8b). For low values of Da_m^R, the conversion of A is very poor as very little B enters the raffinate phase during its time of residence in the stirred cell. The selectivity to C, however, is very close to unity as the small amount of B that enters the raffinate phase is almost entirely consumed by the desired reaction. As Da_m^R increases, conversion increases as an increasing amount of B enters the raffinate phase, but the selectivity drops as increasing amounts of B and C take part in the undesired reaction. In the limit of high Da_m^R and Da_r^R, both the phases of the stirred cell are in phase and reaction equilibrium, and equilibrium performance limits are obtained.

Thus, operating near thermodynamic equilibrium limit results in higher conversion of A but poor selectivity to C. On the other hand, operating under severe kinetic and mass-transfer limitations results in extremely good selectivity to C but very poor conversion of A.

Effect of relative rates of the desired and the undesired reactions

In general, the forward reaction rate constants of the two reactions are not the same. Let us now investigate the effect of the relative forward rates of the desired and undesired reactions on the stirred cell performance.

Figure 9a shows conversion of A and selectivity to C as a function of the ratio $Da_{r_{22}}^R/Da_{r_{11}}^R$ for high Da_m^R (100) for operation in the mass-transfer-controlled regime ($Da_{r_{11}}^R/Da_m^R = 100$) and in the reaction-controlled regime ($Da_{r_{11}}^R/Da_m^R = 0.01$). Da_m^E is fixed at 100. Figure 9b shows the departure of the bulk raffinate composition from reaction equilibrium compositions corresponding to each of the reactions. As indicated in Figure 9b, in the mass-transfer-controlled regime, both reactions are in equilibrium in the bulk raffinate phase. Hence, conversion and selectivity remain relatively constant over the range of $Da_{r_{22}}^R/Da_{r_{11}}^R$ considered (Figure 9a). Furthermore, the values of conversion and selectivity are close to their equilibrium thermodynamic limits (Figure 7), because at high Damköhler numbers, both reactions and mass transfer are relatively faster than product removal.

In the reaction-controlled regime, mass transfer is much faster than both reactions over the range of $Da_{r_{22}}^R/Da_{r_{11}}^R$ considered. For $Da_{r_{22}}^R/Da_{r_{11}}^R > 1$, the desired reaction controls; for $Da_{r_{22}}^R/Da_{r_{11}}^R < 1$, the undesired reaction controls. Therefore, for high values of $Da_{r_{22}}^R/Da_{r_{11}}^R$, the undesired reaction is close to reaction equilibrium, while the desired reaction shows considerable departure from reaction equilibrium. As $Da_{r_{22}}^R/Da_{r_{11}}^R$ decreases, the desired reaction slowly starts to move toward reaction equilibrium, while the undesired reaction starts to deviate from reaction equilibrium. As a result, we observe a decrease in conversion of A and an increase in selectivity to C as $Da_{r_{22}}^R/Da_{r_{11}}^R$ decreases: that is, the undesired reaction becomes less significant than the desired reaction.

Figures 9c and 9d show similar results for low Da_m^R (10). Again, the effect of relative rates of the two reactions is negligible in the mass-transfer-controlled regime and shows the same trends as before in the reaction-controlled regime. In this case, however, the conversions are very low and selectivities are close to unity, because both reactions and mass transfer are much slower than product removal. For different values of $Da_{r_{22}}^R/Da_{r_{11}}^R$, $Da_{r_{11}}^R/Da_m^R$, and Da_m^R, more complicated interactions between the two reactions and mass transfer may be observed.

Effect of off-diagonal terms on conversion and selectivity

We assumed $\mathbf{Da}_m^R$ and $\mathbf{Da}_m^E$ to be diagonal to make interpretation of the results easier. However, the effect of off-diagonal terms on conversion and selectivity can be quite significant. Figure 10 shows the conversion and selectivity as a function of $Da_{r_{11}}^R$ (with $Da_{r_{22}}^R = 10Da_{r_{11}}^R$) for various values of $\mathbf{Da}_m^R$ and $\mathbf{Da}_m^E$. As before, we observe the trade-off between conversion and selectivity. However, due to the presence of the off-diagonal elements, the flux of each component across the interface is governed by the composition gradients of all components in the reacting mixture. Accordingly, the specific values of conversion and selectivity for a given $\mathbf{Da}_r^R$ can differ significantly for various sets of $\mathbf{Da}_m^R$ and $\mathbf{Da}_m^E$.

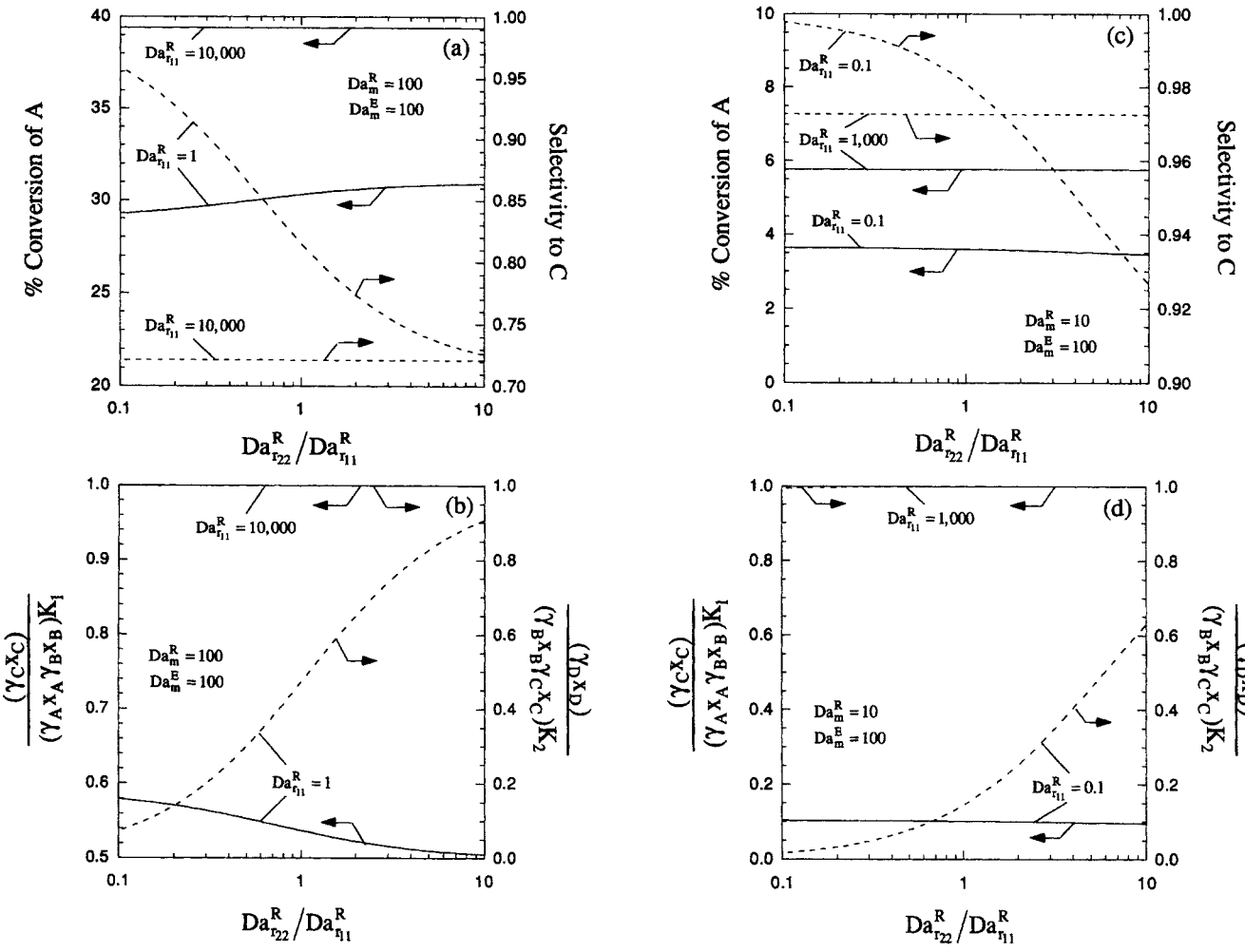

Figure 9. Effect of relative rates of desired and undesired reactions on the performance of the stirred cell.

(a) Conversion and selectivity for $Da^R_m = 100.0$; (b) departure of the bulk raffinate composition from reaction equilibrium for $Da^R_m = 100.0$; (c) conversion and selectivity for $Da^R_m = 10.0$; (d) departure of the bulk raffinate composition from reaction equilibrium for $Da^R_m = 10.0$.

Systems with Solvent-Induced Phase Separation

A suitable solvent that is partially miscible with one or more reactants or products can be added to improve yields and selectivities of desired products, and ease separation of byproducts. Several such examples are presented in Samant and Ng (1998a). In this section, we analyze the effects of reaction kinetics and mass transfer on two of these examples.

Example III: Improvement in Yield

Consider a system with the following reaction:

$$A \Leftrightarrow B \tag{41}$$

where the reaction rate per mole of liquid mixture of composition $\boldsymbol{x}$ is given by

$$r(\boldsymbol{x}) = k_f\left(\gamma_A x_A - \frac{\gamma_B x_B}{K}\right) \tag{42}$$

Solvent I, completely miscible with the product B but only partially miscible with the reactant A, can be used to improve the yield of B:

$$\text{Yield of } B = \frac{\text{Amount of } B \text{ Produced}}{\text{Amount of } A \text{ Fed}} \tag{43}$$

The phase diagram for such a system and its description are available elsewhere (Samant and Ng, 1998a) and the thermodynamic parameters are listed in Table 3.

Let us consider the stirred cell with input streams of pure A ($z^F_A = 1.0$, $F = 1.0$) and pure I ($z^S_I = 1.0$, $S = 1.0$). The yield of B from the stirred cell is now governed by

$$\boldsymbol{Da}^{\phi}_r = [Da^{\phi}_r], \quad \boldsymbol{Da}^{\phi}_m = \begin{bmatrix} Da^{\phi}_{m_{AA}} & Da^{\phi}_{m_{AI}} \\ Da^{\phi}_{m_{IA}} & Da^{\phi}_{m_{II}} \end{bmatrix}, \quad \phi = R, E \tag{44}$$

The yield of B at phase and reaction equilibrium is 91.12% (thermodynamic limit); the yield of a single-phase process is 21.364% (Samant and Ng, 1998a). It should be noted that a single-phase process will also, in general, suffer from kinetic

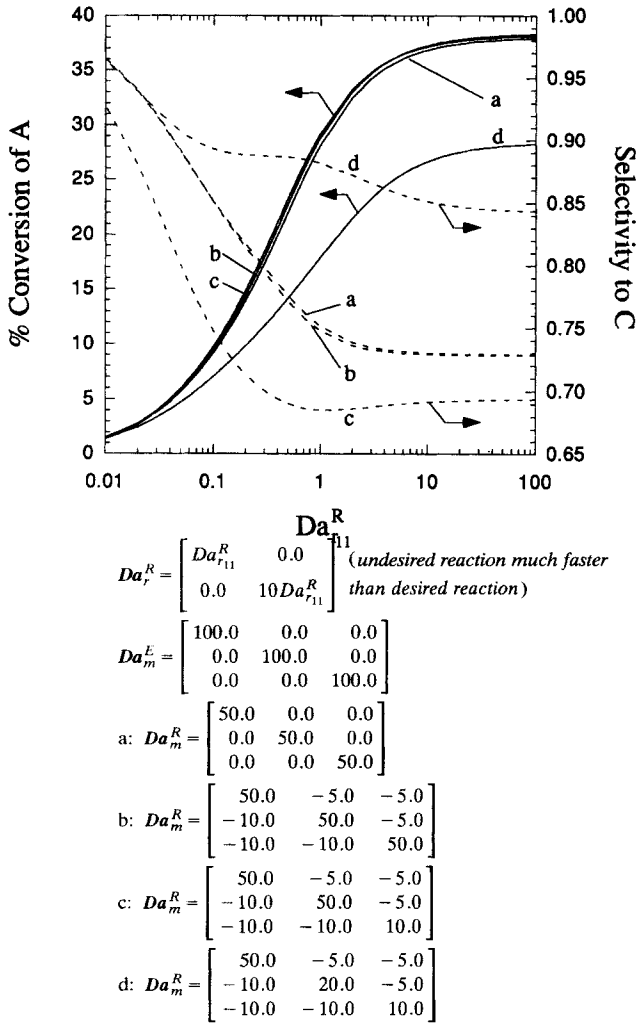

$$\boldsymbol{Da}_r^R = \begin{bmatrix} Da_{r_{11}}^R & 0.0 \\ 0.0 & 10Da_{r_{11}}^R \end{bmatrix}$$ (*undesired reaction much faster than desired reaction*)

$$\boldsymbol{Da}_m^E = \begin{bmatrix} 100.0 & 0.0 & 0.0 \\ 0.0 & 100.0 & 0.0 \\ 0.0 & 0.0 & 100.0 \end{bmatrix}$$

a: $$\boldsymbol{Da}_m^R = \begin{bmatrix} 50.0 & 0.0 & 0.0 \\ 0.0 & 50.0 & 0.0 \\ 0.0 & 0.0 & 50.0 \end{bmatrix}$$

b: $$\boldsymbol{Da}_m^R = \begin{bmatrix} 50.0 & -5.0 & -5.0 \\ -10.0 & 50.0 & -5.0 \\ -10.0 & -10.0 & 50.0 \end{bmatrix}$$

c: $$\boldsymbol{Da}_m^R = \begin{bmatrix} 50.0 & -5.0 & -5.0 \\ -10.0 & 50.0 & -5.0 \\ -10.0 & -10.0 & 10.0 \end{bmatrix}$$

d: $$\boldsymbol{Da}_m^R = \begin{bmatrix} 50.0 & -5.0 & -5.0 \\ -10.0 & 20.0 & -5.0 \\ -10.0 & -10.0 & 10.0 \end{bmatrix}$$

Figure 10. Effect of off-diagonal terms in $\boldsymbol{Da}_m^R$ on the performance of the stirred cell.

limitations. Hence this is the maximum possible yield that can be obtained from a single-phase process.

Let us begin our analysis by assuming diagonal $\boldsymbol{Da}_m^R$ and $\boldsymbol{Da}_m^E$ with equal mass-transfer coefficients of all components ($Da_{m_{AA}}^{\phi} = Da_{m_{BB}}^{\phi} = Da_m^{\phi}$, $\phi = R$, E), and high Da_m^E (100). Figure 11 shows the yield of B as a function of Da_r^R/Da_m^R for

Table 3. Thermodynamic Parameters for Example III

Temp. = 298.15 K; Pres. = 1 atm; Equil. Const., $K = 0.5$		
UNIQUAC Equation Parameters (Sorenson and Arlt, 1979)		
Pure Component Parameters		
Component	r	q
A (3)	2.204	2.072
B (1)	0.92	1.4
I (2)	6.2873	4.48
Binary Interaction Parameters (K)		
a (1,1) = 0.0	a (1,2) = −210.21	a (1,3) = 17.465
a (2,1) = −9.5328	a (2,2) = 0.0	a (2,3) = 259.82
a (3,1) = 104.02	a (3,2) = 662.44	a (3,3) = 0.0

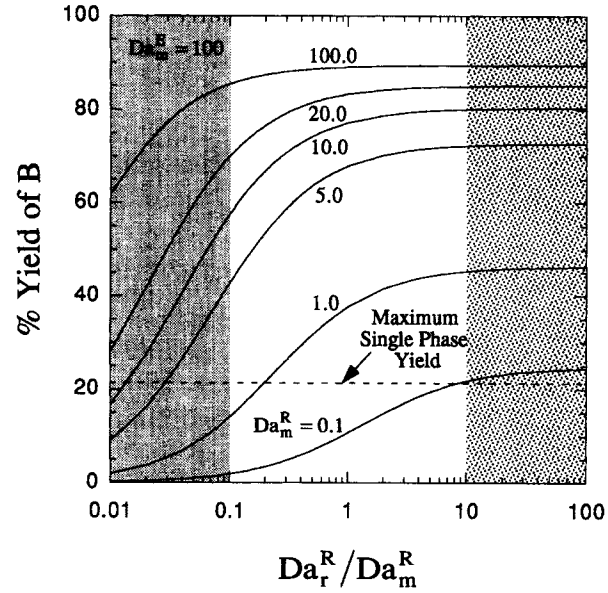

Figure 11. Effect of kinetics and mass transfer on the yield of B.

values of Da_m^R ranging from 0.1 to 100. The yield increases with Da_r^R/Da_m^R as we go from the reaction-controlled regime to the mass-transfer-controlled regime for all Da_m^R. In the mass-transfer-controlled regime, the bulk raffinate phase is in reaction equilibrium. Hence, the yield reaches its equilibrium value and does not increase with further increase in Da_r^R/Da_m^R. For any Da_r^R/Da_m^R, the yield is higher for higher values of Da_m^R, as rates of mass transfer and reaction relative to the rate of product removal are higher. In the limit of high Da_m^R and Da_r^R, the yield tends to the thermodynamic limit. It should be noted that for very low values of Da_m^R (< 0.1) the yield is always lower than the maximum yield from a single-phase process. Hence, the addition of solvent I may not always be beneficial.

Figure 12 shows the effect of off-diagonal terms in $\boldsymbol{Da}_m^R$ and $\boldsymbol{Da}_m^E$ on the yield of B. Curve a represents the case where $\boldsymbol{Da}_m^R$ and $\boldsymbol{Da}_m^E$ are diagonal. The off-diagonal terms may have an adverse effect on the yield (curves a and b) or may lead to further improvement in yield (curves b and c). If the off-diagonal terms significantly enhance the flux of B out of the raffinate phase, yields higher than the thermodynamic limit of 91.12% can be obtained for high Da_r^R (curves c and d). As expected, additional resistance to mass transfer in extract phase leads to reduced yields (in the order of curves c, d and e).

Figure 13a shows the flowsheet for a simple process for improvement in the yield of B by addition of solvent I. The stirred-cell model represents the single-stage extractive reactor (RE). The raffinate stream is recycled. The solvent I is separated from the extract stream and recycled. Figure 13b shows the yield of B as a function of Da_r^R for some of the $\boldsymbol{Da}_m^R$ and $\boldsymbol{Da}_m^E$ values considered in Figure 12. Small amounts of B and I enter the feed stream through the recycled raffinate stream. Hence, the yield from the flowsheet is slightly different. Again, it is interesting to note that for some parameter values, yields in excess of the thermodynamic limit can be obtained (curve c).

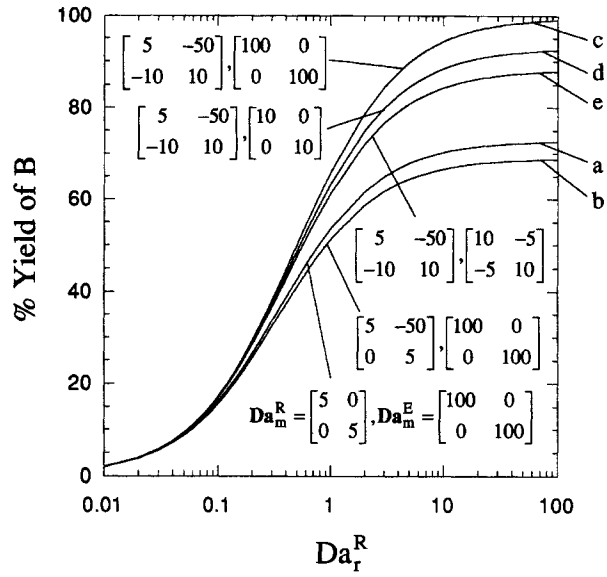

Figure 12. Effect of off-diagonal terms in Da_m^R and Da_m^E on the yield of B.

In the thermodynamic limit, the raffinate and extract phases are in reaction and phase equilibrium with each other. Therefore, the system has 3(components)-1(reaction)-2(phases) = 0 degrees of freedom at constant temperature and pressure. Thus, in the thermodynamic limit, we cannot use a multistage extractive reactor. It is for this reason that we used a single-stage extractive reactor in the flowsheet of Figure 13a. For kinetically-constrained or mass-transfer-constrained systems, however, the bulk raffinate and extract phases are not in reaction equilibrium or in phase equilibrium with each other. Therefore, by using the additional degrees of freedom now available, a multistage extractive reactor can be used to further improve the yield of B.

Example IV: Improvement in Selectivity

Consider a system with reactions in series

$$A \Leftrightarrow B + C \Leftrightarrow D \tag{45}$$

or with reactions in parallel

$$\begin{aligned} A &\Leftrightarrow B + C \\ A &\Leftrightarrow D \end{aligned} \tag{46}$$

In both cases, the first reaction is the desired reaction, and the second reaction is undesired. Note that these two systems are equivalent in the thermodynamic limit because of reversibility. However, the reaction rates for the reactions in series are given by

$$\begin{aligned} r_1(x) &= k_{f_1}\left(\gamma_A x_A - \frac{\gamma_B x_B \gamma_C x_C}{K_1}\right), \\ r_2(x) &= k_{f_2}\left(\gamma_B x_B \gamma_C x_C - \frac{\gamma_D x_D}{K_2}\right) \end{aligned} \tag{47}$$

and for the reactions in parallel by

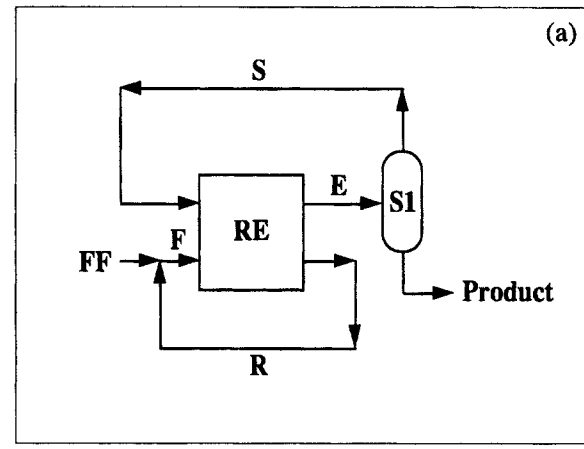

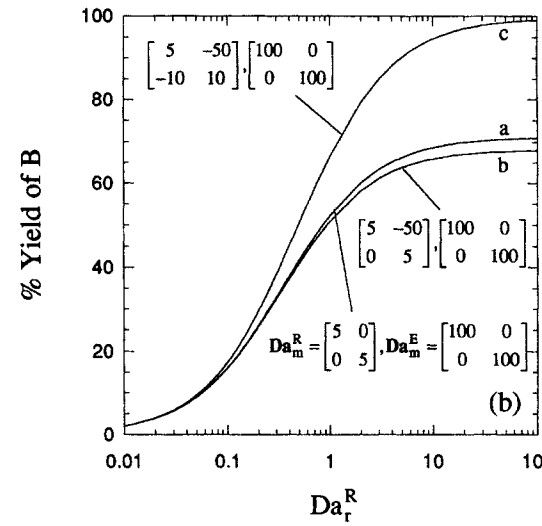

Figure 13. (a) Process for improvement in the yield of B; (b) effect of kinetics and mass transfer on the yield of B.

$$\begin{aligned} r_1(x) &= k_{f_1}\left(\gamma_A x_A - \frac{\gamma_B x_B \gamma_C x_C}{K_1}\right), \\ r_2(x) &= k_{f_2}\left(\gamma_A x_A - \frac{\gamma_D x_D}{K_2}\right) \end{aligned} \tag{48}$$

Hence, the effects of reaction kinetics and mass transfer on these systems will be different. In both cases, the performance parameter of interest is the product distribution:

$$\text{Product Distribution} = \frac{\text{Total } B \text{ Produced}}{\text{Total } A \text{ Reacted}} \tag{49}$$

The product distribution can be greatly improved by employing a solvent I, which is miscible with A, C, and D, but partially miscible with B (Samant and Ng, 1998a). The thermodynamic data for this five-component system with two reactions and the corresponding phase diagram in transformed mole fraction coordinates are presented elsewhere (Samant and Ng, 1998b). At constant temperature and pressure, the system has 5(components)-2(reactions)-2(phases) = 1 degree of freedom. Hence, a multistage extractive reactor (MSER) is

a natural choice for obtaining significant improvements in product distribution over the single-phase process (Samant and Ng, 1998a,b). Here, the effects of kinetics and mass transfer on a single-stage process are demonstrated.

Let us consider the stirred cell with input streams of pure A ($z_A^F = 1.0$, $F = 1.0$) and pure I ($z_I^S = 1.0$, $S = 1.5$). For this system, we refer to the A-rich phase as the raffinate phase and the A-lean phase as the extract phase. The yield of B from the stirred cell is governed by

$$\mathbf{Da}_r^{\phi} = \begin{bmatrix} Da_{r_{11}}^{\phi} & 0.0 \\ 0.0 & Da_{r_{22}}^{\phi} \end{bmatrix},$$

$$\mathbf{Da}_m^{\phi} = \begin{bmatrix} Da_{m_{AA}}^{\phi} & Da_{m_{AB}}^{\phi} & Da_{m_{AC}}^{\phi} & Da_{m_{AI}}^{\phi} \\ Da_{m_{BA}}^{\phi} & Da_{m_{BB}}^{\phi} & Da_{m_{BC}}^{\phi} & Da_{m_{BI}}^{\phi} \\ Da_{m_{CA}}^{\phi} & Da_{m_{CB}}^{\phi} & Da_{m_{CC}}^{\phi} & Da_{m_{CI}}^{\phi} \\ Da_{m_{IA}}^{\phi} & Da_{m_{IB}}^{\phi} & Da_{m_{IC}}^{\phi} & Da_{m_{II}}^{\phi} \end{bmatrix}, \quad \phi = R, E \tag{50}$$

In the thermodynamic limit, the product distribution at phase and reaction equilibrium is 0.6052. Also, the equilibrium product distribution of a single-phase process is 0.3842. Here again, the single-phase process may also suffer from kinetic limitations.

Let us begin with a case where the forward reaction rate constants for both reactions are the same ($Da_{r_{11}}^R = Da_{r_{22}}^R =$ that is, $i\,Da_r^R$), $\mathbf{Da}_m^R$ and $\mathbf{Da}_m^E$ are diagonal, and mass-transfer coefficients for all components are the same ($Da_{m_{ii}}^{\phi} = Da_m^{\phi}$, i, $= A, B, C, I$, $\phi = R, E$). Figure 14a shows the performance of the stirred cell in terms of conversion of A and selectivity to the desired product C as a function of the ratio Da_r^R/Da_m^R for various values of Da_m^R for the reactions in series. As Da_r^R/Da_m^R increases, conversion of A increases from zero (for $Da_r^R = 0$) and the product distribution decreases from unity (for $Da_r^R = 0$) to equilibrium values. These equilibrium values are reached in the mass-transfer-controlled regime where the bulk raffinate phase is in reaction equilibrium. In the reaction-controlled regime, both reactions are slower than mass transfer. Hence, the transfer of I into the raffinate phase and transfer of B (as it is partially miscible with I) out of the raffinate phase are extremely rapid in comparison to the reactions. Since the reactions take place only in the raffinate phase, this results in high values of product distribution. The total conversion of A, however, is very low as the reactions are very slow. Therefore, a trade-off between conversion and product distribution similar to that observed in Example II is observed. As expected, the trade-off is more pronounced for low values of Da_m^R. In the limit of high Da_r^R and Da_m^R, the conversion and product distribution tend to their thermodynamic equilibrium limits.

Figure 14b shows the performance of the stirred cell for the reactions in parallel. In this case, as we move from the reaction-controlled regime to the mass-transfer-controlled regime, conversion of A and product distribution both increase from zero (for $Da_r^R = 0$) to their equilibrium values. These equilibrium values are reached in the mass-transfer-controlled regime. Both the conversion and product distribution increase in the same direction, because in the parallel

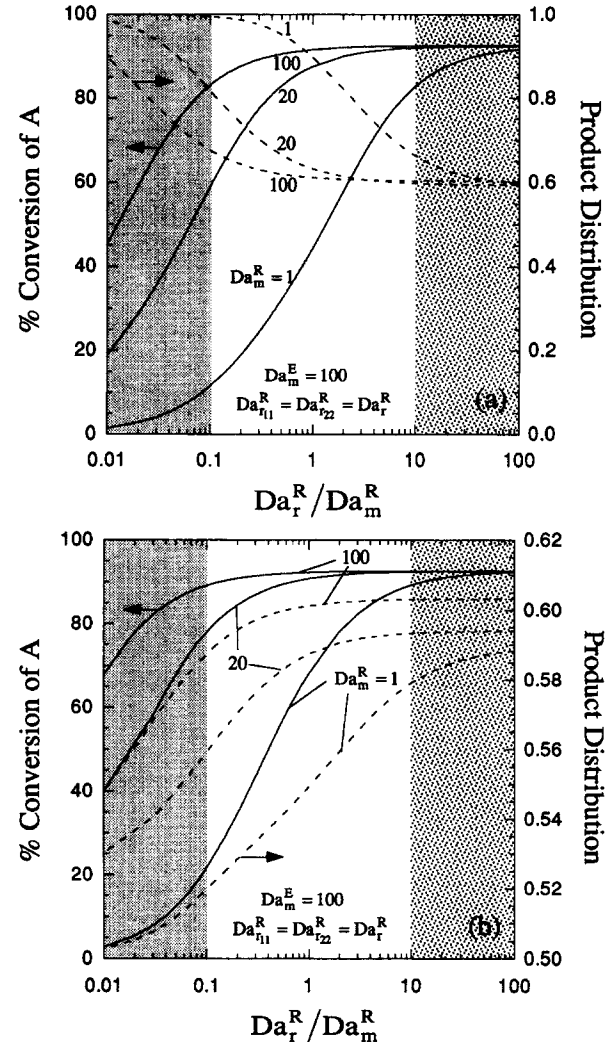

Figure 14. (a) Performance of the stirred cell for reactions (a) in series; (b) in parallel.

reaction scheme of Eq. 43, reactant A takes part in both the reactions and the desired product B, and C is not involved in the undesired reaction. The conversion and product distribution both increase with increasing Da_m^R, as the rates of mass transfer and of both reactions increase in comparison to the rate of product removal. Again, in the limit of high Da_r^R and Da_m^R, the conversion and product distribution tend to their thermodynamic equilibrium limits. These limits are the same for both reaction schemes, because they are completely equivalent at phase and reaction equilibrium. As the trade-off between conversion and product distribution does not exist in this case, it is beneficial to operate near the equilibrium thermodynamic limit.

Choice of Reactor Attributes

Extractive reaction processes are used to improve yields of desired products, selectivities to desired products, and ease of separation of byproducts. In some applications, even small percentage improvements in yield or selectivity can be extremely significant economically. Therefore, to achieve the desired performance objectives, it is necessary to carefully

choose the ideal reactor configuration. Some of the important reactor attributes to be considered are:

- Choice of dispersed and continuous phases
- Mean droplet size of dispersed phase
- Dispersed and continuous phase holdups
- Residence time or reactor size.

As discussed in the examples above, the effects of kinetics and mass transfer can be parametrized by Damköhler number matrices for reaction and mass transfer (Eqs. 27 and 28). These matrices can be recast as follows:

$$Da^{\phi}_{r_{pp}} = Y\tau_{\phi}k_{f_p}, \qquad Da^{\phi}_{r_{pq(p\neq q)}} = 0 \qquad p,q = 1, 2, \ldots, r; \quad \phi = R, E \tag{51}$$

$$Da^{\phi}_{m_{ij}} = \tau_{\phi}a^{\phi}_{s}K^{I\phi}_{m_{ij}}, \qquad i,j = 1, 2, \ldots, c-1; \quad \phi = R, E \tag{52}$$

For clarity of discussion, assume that the reaction takes place in only one of the phases, $\boldsymbol{Da}^{\phi}_{m}$ are diagonal, and mass-transfer coefficients of all components are equal ($Da^{\phi}_{m_{ii}} = Da^{\phi}_{m}$). For the reactive phase (denoted as X), we can write:

$$Da^{X}_{r_{pp}} = \tau_X k_{f_p}, \qquad p = 1, 2, \ldots, r$$

$$Da^{X}_{m} = \tau_X a^{X}_{s}K^{IX}_{m} \tag{53}$$

Therefore,

$$\frac{Da^{X}_{r_{pp}}}{Da^{X}_{m}} = \frac{1}{a^{X}_{s}}\frac{k_{f_p}}{K^{IX}_{m}}, \qquad p = 1, 2, \ldots, r \tag{54}$$

To achieve the desired performance objectives from an extractive reaction process, a proper choice of these Damköhler numbers is necessary. A summary of these choices for the various cases considered in Examples II, III and IV is presented in Table 4. Equations 53 and 54 relate the Damköhler numbers to reactor attributes (a^{X}_{s}, τ_X) and physical and chemical properties of the system (k_{f_p}, K^{IX}_{m}); and form the basis for selection of reactor attributes. We choose reactor attributes in such a way as to keep the values of the Damköhler number matrices in the desired range. Since the ratio $Da^{X}_{r_{pp}}/Da^{X}_{m}$ does not depend on the residence time of the reactive phase (τ_X), it is used to choose phase attributes such as the choice of the dispersed and continuous phases, mean droplet size of the dispersed phase, and fractional holdups of dispersed and continuous phases. Then, Da^{X}_{m} (or $Da^{X}_{r_{pp}}$) is used to fix the residence time (reactor volume). The choices of a^{X}_{s} and τ_X, necessary to achieve the desired combinations of $Da^{X}_{r_{pp}}/Da^{X}_{m}$ and Da^{X}_{m} values, are given in Table 5.

The specific surface area of the reactive phase (a^{X}_{s}) is the key variable that is used to choose the phase attributes. a^{X}_{s}

Table 4. Damköhler Number Choices for Examples II, III and IV

Examples	Da^{R}_{r}/Da^{R*}_{m}	Da^{R}_{m}	Objective
II:			
$\frac{Da^{R}_{r_{22}}}{Da^{R}_{r_{11}}} = 0.1$ (Figures 9a and 9c)	Low (< 0.1)	High (~ 100)	• Trade-off between conversion and selectivity
$\frac{Da^{R}_{r_{22}}}{Da^{R}_{r_{11}}} = 1.0$ (Figure 8a)	Low (< 0.1)	High (~ 100)	• Trade-off between conversion and selectivity
$\frac{Da^{R}_{r_{22}}}{Da^{R}_{r_{11}}} = 10.0$ (Figures 9a and 9c)	High (> 100)	Low (~ 20)	• Trade-off between conversion and selectivity
III:			
Figure 11	High (> 10)	High (> 100)	• High yield
IV:			
Reactions in series: Figure 14a	Low (< 0.1)	High (~ 100)	• Trade-off between conversion and selectivity
Reactions in parallel: Figure 14b	High (> 10)	High (~ 100)	• High yield and selectivity

*For multiple reactions (Examples II and IV), $Da^{R}_{r} = Da^{R}_{r_{11}}$.

Table 5. Choices of a^{X}_{s} and τ_X for Desired Values of Da^{X}_{r}/Da^{X}_{m} and Da^{X}_{m}

Desired Da^{X}_{r}/Da^{X}_{m}	Given k_f/K^{IX}_{m}	Targeted a^{X}_{s} (Based on Eq. 54)	Desired Da^{X}_{m}	Targeted τ_X (Based on Eq. 53)
Low	Low	High	Low	• Decrease τ_X (use smaller reactors).
			High	• High a^{X}_{s} will give high Da^{X}_{m}. • Increase τ_X if necessary.
Low	High	High	Low	• Decrease τ_X (use smaller reactors).
			High	• High a^{X}_{s} will give high Da^{X}_{m}. • Increase τ_X if necessary.
High	Low	Low*	Low	• Low a^{X}_{s} will give low Da^{X}_{m}. • Decrease τ_X if necessary.
			High	• Increase τ_X.
High	High	Highest Possible**	Low	• Decrease τ_X if necessary.
			High	• Highest possible a^{X}_{s} will give highest possible Da^{X}_{m}. • Increase τ_X if necessary.

*For lower values of a^{X}_{s}, higher values of τ_X (larger reactors) are needed to achieve any value of Da^{X}_{m}.
**For high k_f/K^{IX}_{m}, we can get sufficiently high values of Da^{X}_{r}/Da^{X}_{m} without having to use low values of a^{X}_{s} (and hence larger reactors). Hence we try to use the highest possible value of a^{X}_{s} in order to keep τ_X as low as possible.

Table 6. Reactor Attributes for Examples II, III and IV

Examples	k_f/K_m^{IX*}	a_s^X	Reactor Attributes
II:			
$\frac{Da_{r_{22}}^R}{Da_{r_{11}}^R} = 0.1$	Low/High	High	• Disperse reactive phase. • Use small mean droplet size.
$\frac{Da_{r_{22}}^R}{Da_{r_{11}}^R} = 1.0$	Low/High	High	• Disperse reactive phase. • Use small mean droplet size.
$\frac{Da_{r_{22}}^R}{Da_{r_{11}}^R} = 10.0$**	Low	Low	• Disperse nonreactive phase. • Use large mean drop size.
	High	Low	• Disperse nonreactive phase. • Use large mean drop size.
III	Low	Low	• Disperse nonreactive phase. • Use large mean drop size. • Use larger reactor.
	High	Highest Possible	• Disperse reactive phase. • Use mean drop size that gives highest possible a_s^X.
IV			
Reactions in series	Low/High	High	• Disperse reactive phase. • Use small mean droplet size.
Reactions in parallel	Low	Low	• Disperse nonreactive phase. • Use large mean drop size. • Use larger reactor.
	High	Highest Possible	• Disperse reactive phase. • Use mean drop size that gives highest possible a_s^X.

*For multiple reactions (Examples II and IV), $k_f = k_{f_1}$.
**Similar observations were made by Doraiswami and Yesuda (1996).

can be qualitatively correlated to the phase attributes with the aid of the following observations.

- For liquid-liquid reactors, typically, $V^{\text{disp}} < V^{\text{cont}}$ and $a_s^{\text{disp}} > a_s^{\text{cont}}$. Therefore, for high values of a_s^X, we disperse the reactive phase (X = disp); for low values of a_s^X, we disperse the nonreactive phase (X = cont).
- Both a_s^{disp} and a_s^{cont} increase with decreasing mean droplet size for fixed-phase holdups.
- a_s^X increases with decrease in the fractional volumetric holdup of the reactive phase.

With these observations in mind, phase attributes can be easily selected. Table 6 summarizes the decisions derived from Tables 4 and 5 for Examples II, III and IV.

While the above discussion is qualitative in nature, quantitative analysis can easily be carried out for specific cases if all physical properties of the system under consideration are known. Some practical considerations, however, override the decisions arrived at above. It is thus advisable to disperse corrosive liquid to avoid contact with reactor walls and to use small holdups of hazardous material, even if this is contrary to the conclusions arrived at above. However, if one of the reactor attributes is changed, others can be manipulated suitably to get as close to the desired Damköhler number values as possible.

Conclusions

Performance of liquid-liquid extractive reaction processes that are controlled by kinetics and/or mass transfer can differ significantly from the equilibrium thermodynamic limit. A model, which captures the essential features of thermodynamic nonidealities and multicomponent mass transfer, is derived to elucidate the interplay of these factors. As demonstrated, the performance of extractive reactors can be parametrized by Damköhler number matrices for reaction and mass transfer. Damköhler numbers for reaction and mass transfer compare the characteristic residence time to the characteristic times of reaction and mass transfer, respectively. The Damköhler number for mass transfer does not follow the conventional definition which is based on a closed system; instead, it signifies the time required for sufficient mass transfer to take place in an open system. The ratio of these Damköhler numbers is the conventional Damköhler number for mass transfer and represents the relative rates of reaction and mass transfer. The off-diagonal terms in Damköhler number matrices for mass transfer, which arise from thermodynamic nonidealities, were shown to significantly affect the performance of extractive reactors.

In addition to the insights, the model and the accompanying analysis can be used in process design and development as follows. First, we determine the values of Damköhler numbers for mass transfer and the Damköhler number ratio that gives the desired performance. Then, based on the heuristics developed in this work, reactor attributes such as choice of dispersed and continuous phases, drop size, phase holdups, and residence time are selected to obtain these values. The ability to manipulate the reactor attributes to obtain the desired performance will allow greater flexibility in the design of extractive reaction processes.

Acknowledgment

The support of the National Science Foundation (Grant No. 9807101) for this research is gratefully acknowledged.

Notation

a = total interfacial surface area for mass transfer, m^2
a_s = specific interfacial surface area for mass transfer, 1/m
A, A_i, B, C, D, I = generic chemical species
B_{ij} = i-j the element of inverted Maxwell-Stefan diffusivity matrix, s/m^2
c = number of components
c_p = number of products
c_r = number of reactants
c_T = total liquid phase concentration, mol/m^3
$\boldsymbol{Da}_m^{\phi}$ = matrix of Damköhler numbers for mass transfer for phase ϕ
$\boldsymbol{Da}_r^{\phi}$ = matrix of Damköhler numbers for reaction in phase ϕ
E_i = enhancement factor for mass transfer of component i across the interface
F, S, E, R = molar flow rates of feed, solvent, extract, and raffinate streams, mol/s
ΔG_i = standard Gibbs free energy change of reaction i
Ha = Hatta number
H_E = molar holdup in the extract phase, mol
H_R = molar holdup in the raffinate phase, mol
$\bar{J}_i$ = molar flux of component i relative to the molar average velocity, mol/$m^2 \cdot$s
$\bar{J}_T$ = total molar flux relative to the molar average velocity, mol/$m^2 \cdot$s
$\boldsymbol{k}_f$ = matrix of forward reaction rate constants (Eq. 26)
k_{f_i} = forward reaction rate constant of reaction i, 1/s
k_{r_i} = reverse reaction rate constant of reaction i, 1/s
K_i = thermodynamic equilibrium constant of reaction i

$K^I_{m_{ij}}$ = coefficient for mass transfer of component i across the interface due to the gradient in composition of component j, m/s
$\overline{N}_i$ = molar flux of component i relative to stationary coordinates, mol/m^2·s
$\overline{N}_T$ = total molar flux relative to stationary coordinates, mol/m^2·s
P = pressure, atm
r = number of reactions
r_i = rate of reaction i
R_g = universal gas constant
T = temperature, K
V^{cont} = volume of continuous phase, m^3
V^{disp} = volume of dispersed phase, m^3
x_i = mole fraction of component i
X_i = transformed mole fraction of component i
Δx_i^R = composition difference in the raffinate phase
Δx_i^E = composition difference in the extract phase
Y = binary integer parameter
z_i^F = mole fraction of component i in the feed stream
z_i^S = mole fraction of component i in the solvent stream
β^ϕ = mole fraction matrix (Eq. 17) for phase ϕ
γ_i = activity coefficient of component i
Γ_{ij} = i-jth element of matrix of dimensionless thermodynamic factors
κ_{ij} = Maxwell-Stefan i-j pair mass transfer coefficient, m/s
μ_i = chemical potential of component i
$\upsilon_{i,m}$ = stoichiometric coefficient of component i in reaction m
$\upsilon_{\text{TOT},m}$ = algebraic sum of the stoichiometric coefficients of the components in reaction m
Φ = Thiele modulus

Subscripts

i, j, k, m, p, q = indices

Superscripts

cont = continuous phase
disp = dispersed phase
E = in the extract phase
I = at the interface
R = in the raffinate phase
X = in the reactive phase
ϕ = phase index

Literature Cited

Anderson, W. K., and T. Veysoglu, "A Simple Procedure for the Epoxidation of Acid Sensitive Olefinic Compounds with *m*-Chlorperbenzoic Acid in an Alkaline Biphasic Solvent System," *J. Org. Chem.*, **38**, 2267 (1973).

Berry, D. A., and K. M. Ng, "Synthesis of Reactive Crystallization Processes," *AIChE J.*, **43**, 1737 (1997).

Chapman, T. W., "Extraction—Metals Processing," *Handbook of Separation Process Technology*, R. W. Rousseau, ed., Wiley, New York (1987).

Coca, J., G. Adrio, C. Y. Jeng, and S. H. Langer, "Gas and Liquid Chromatographic Reactors," *Preparative and Production Scale Chromatography*, G. Ganestos and P. E. Barker, eds., Marcel Dekker, New York (1993).

DeGarmo, J. L., V. N. Parulekar, and V. Pinjala, "Consider Reactive Distillation," *Chem. Eng. Prog.*, **88**, 43 (1992).

Doherty, M. F., and G. Buzad, "Reactive Distillation by Design," *Trans. IChemE*, **70**, 448 (1992).

Doraiswami, R., and K. E. Yesuda, "Maximizing Selectivity of Liquid-Liquid Reaction Systems. Control of the Dispersion Process," *Chem. Eng. Comm.*, **147**, 119 (1996).

Frank, M. J. W., J. A. M. Kuipers, G. F. Versteeg, and W. P. M. Van Swaaij, "Modelling of Simultaneous Mass and Heat Transfer with Chemical Reaction Using the Maxwell-Stefan Theory: I. Model Development and Isothermal Study," *Chem. Eng. Sci.*, **50**, 1645 (1995).

King, C. J., *Separation Processes*, 2nd ed., McGraw-Hill, New York (1980).

King, M. L., A. L. Forman, C. Orella, and S. H. Pines, "Extractive Hydrolysis for Pharmaceuticals," *Chem. Eng. Prog.*, **81**, 36 (1985).

Krishna, R., and G. Standart, "A Multicomponent Film Model Incorporating an Exact Matrix Method of Solution to the Maxwell-Stefan Equations," *AIChE J.*, **22**, 383 (1976).

Krishna, R., "A Generalized Film Model for Mass Transfer in Non-Ideal Fluid Mixtures," *Chem. Eng. Sci.*, **32**, 659 (1977).

Krishna, R., "A Note on the Film and Penetration Models for Multicomponent Mass Transfer," *Chem. Eng. Sci.*, **33**, 765 (1978).

Krishna, R., and R. Taylor, "Multicomponent Mass Transfer: Theory and Applications," *Handbook of Heat and Mass Transfer*, Vol. 2, N. P. Cheremisinoff, ed., Gulf Publishing Co., Houston (1986).

Krishna, R., and S. T. Sie, "Strategies for Multiphase Reactor Selection," *Chem. Eng. Sci.*, **49**, 4029 (1994).

Krishna, R., and J. A. Wesselingh, "The Maxwell-Stefan Approach to Mass Transfer," *Chem. Eng. Sci.*, **52**, 861 (1997).

Kuntz, E. G., "Homogeneous Catalysis in Water," *Chemtech*, No. 9, 570 (1987).

Mersmann, A., and M. Kind, "Chemical Engineering Aspects of Precipitation from Solution," *Chem. Eng. Tech.*, **11**, 264 (1988).

Pahari, P. K., and M. M. Sharma, "Recovery of Morpholine Via Reactive Extraction," *Ind. Eng. Chem. Res.*, **30**, 2015 (1991).

Samant, K. D., and K. M. Ng, "Synthesis of Extractive Reaction Processes," *AIChE J.*, **44**(6), 1363 (1998a).

Samant, K. D., and K. M. Ng, "Design of Multistage Extractive Reaction Processes," *AIChE J.*, in press (1998b).

Sentarli, I., and A. Hortacsu, "Solution of the Linearized Equations of Multicomponent Mass Transfer with Chemical Reaction and Convection for a Film Model," *Ind. Eng. Chem. Res.*, **26**, 2409 (1987).

Sharma, M. M., "Multiphase Reactions in the Manufacture of Fine Chemicals," *Chem. Eng. Sci.*, **43**, 1749 (1988).

Sherwood, T. K., R. L. Pigford, and C. R. Wilke, *Mass Transfer*, McGraw-Hill, New York (1975).

Sorenson, J. M., and W. Arlt, "Liquid-Liquid Equilibrium Data Collection," *DECHEMA Chemistry Data Ser.*, Vol. 5, Parts 2 and 3, DECHEMA, Frankfurt (1979).

Taylor, R., and R. Krishna, *Multicomponent Mass Transfer*, Wiley, New York (1993).

Tonkovich, A. L. Y., and R. W. Carr, "Modeling of the Simulated Countercurrent Moving-Bed Chromatographic Reactor Used for the Oxidative Coupling of Methane," *Chem. Eng. Sci.*, **49**, 4657 (1994).

Tsotsis, T. T., A. M. Champagnie, R. G. Minet, and P. K. T. Liu, "Catalytic Membrane Reactors," *Computer Aided Design of Catalysts*, R. E. Becker and C. Pereira, eds., Marcel Dekker, New York (1993).

Ung, S., and M. F. Doherty, "Vapor-Liquid Phase Equilibrium in Systems with Multiple Chemical Reactions," *Chem. Eng. Sci.*, **50**, 23 (1995).

Venimadhavan, G., G. Buzad, M. F. Doherty, and M. F. Malone, "Effect of Kinetics on Residue Curve Maps for Reactive Distillation," *AIChE J.*, **40**, 1814 (1994).

Manuscript received Apr. 15, 1998, and revision received July 29, 1998.